Pressure Evolution of the Magnetism and Fermi Surface of YbPtBi Probed by a Tunnel Diode Oscillator Based Method

Y. E. Huang(黄炎恩)[1], F. Wu(吴帆)[1], A. Wang(王安)[1], Y. Chen(陈晔)[1], L. Jiao(焦琳)[1], M. Smidman[1,2], and H. Q. Yuan(袁辉球)[1,2,3,4*]

[1]*Center for Correlated Matter and Department of Physics, Zhejiang University, Hangzhou 310058, China*
[2]*Zhejiang Province Key Laboratory of Quantum Technology and Device, Department of Physics, Zhejiang University, Hangzhou 310058, China*
[3]*State Key Laboratory of Silicon Materials, Zhejiang University, Hangzhou 310058, China*
[4]*Collaborative Innovation Center of Advanced Microstructures, Nanjing 210093, China*

(Received 10 June 2022; accepted manuscript online 25 July 2022)

A central research topic in condensed matter physics is the understanding of the evolution of various phases and phase transitions under different tuning parameters such as temperature, magnetic field and pressure. To explore the pressure-induced evolution of the magnetism and Fermi surface of the heavy fermion antiferromagnet YbPtBi, we performed tunnel diode oscillator based measurements under pressure at low temperatures in high magnetic fields. Our results reveal that the magnetic order strengthens and the Fermi surface shrinks as the pressure increases, which are consistent with typical observations for Yb-based heavy fermion compounds. In addition, an anomalous change in the quantum oscillation amplitudes is observed above 1.5 GPa, and determining the origin requires further study.

DOI: 10.1088/0256-307X/39/9/097101

In strongly correlated electron systems, many body electron–electron interactions lead to a wide range of unusual physical phenomena and emergent behaviors absent in the weakly correlated counterparts. In research of such systems, it is often vitally important to map the properties upon tuning with various non-thermal parameters, which can adjust the balance of competing interactions, allowing for the realization of novel phenomena and unusual electronic phases.[1–5] As such, it is particularly important to be able to perform measurements under a variety of extreme conditions, especially at very low temperatures, high magnetic fields, and high pressures.

The cubic half-Heusler compound YbPtBi is an Yb-based heavy fermion system, which orders antiferromagnetically below $T_{\rm N} = 0.4$ K at ambient pressure, and the heavy fermion behavior is manifested by an extremely large Sommerfeld coefficient of 8 J/(mol·K^2),[6] indicating large effective carrier masses and significant electron correlations. Upon applying a magnetic field, the antiferromagnetic order is suppressed to a quantum critical point (QCP) at about 0.4 T, above which there is an extended region of non-Fermi liquid behavior, before a Fermi liquid ground state onsets above 0.8 T.[7,8] In addition, angle resolved photoemission spectroscopy, transport, and specific heat measurements demonstrate the presence of Weyl fermions, making YbPtBi a rare example of a strongly correlated Weyl semimetal.[9,10] Measurements up to 0.8 GPa show that $T_{\rm N}$ has a slight increase with pressure,[11] but detailed measurements under pressure are lacking.

Here, in order to explore the pressure-induced evolution of the magnetism and Fermi surface, we have performed measurements on YbPtBi using the tunnel-diode oscillator (TDO) based method. The TDO based method[12,13] has been utilized as a sensitive probe of a variety of aspects of condensed matter systems, in particular for measuring the magnetic penetration depth of unconventional superconductors in order to reveal the superconducting pairing states,[14–18] probing the Fermi surface via measurements of quantum oscillations,[19–21] and mapping the phase diagrams of correlated materials.[22,23] The major advantages of this technique are a simple design, high precision, and the ability to perform measurements without the need to attach leads to the sample, avoiding a source of sample stress and contact resistance. In order to expand the range of extreme conditions accessible for the TDO measurements, we have modified the previous design utilized for measurements of the magnetic penetration depth[24] so as to be compatible with measurements at very low temperatures and high magnetic fields. This allows for measurements to be performed down to below 0.1 K, at pressures up to 2.5 GPa.

In this Letter, we provide an overview of measurements using the TDO-based method, focussing on the recent developments which enable us to measure under multiple extreme conditions. We present the results of measurements of YbPtBi down to 0.09 K, under pressures and in applied magnetic fields up to 2.5 GPa and 15 T, respectively. The constructed p–B phase diagram suggests that magnetic order strengthens with increasing pressure. On the other hand, we probe the evolution of the quantum oscillations with pressure, which demonstrates a shrinking of the Fermi surface, consistent with an increasing localization of the $4f$ electrons. In addition, an abrupt change in quantum oscillation amplitudes emerges above 1.5 GPa at around $T_{\rm N}$, whereas there is no significant change in the frequencies. How to understand the anomalous change in the quan-

*Corresponding authors. Email: hqyuan@zju.edu.cn
© 2022 Chinese Physical Society and IOP Publishing Ltd

tum oscillation amplitudes without a reconstruction of the Fermi surface is an intriguing question, and further experiments are necessary to address this problem.

Experimental Setup. The basis of the TDO method is the measurement of the resonant frequency of an RLC circuit, composed of a resistor, inductor and capacitor, where the sample is placed in the coil of the inductor. The change of inductance induced by the sample is reflected in the measured resonant frequency. The I–V curve of a tunnel diode has a region where an increase in the voltage results in a decrease of the current, namely a negative differential resistance. When a voltage bias is applied so that the tunnel diode has a negative differential resistivity, it acts as a negative alternating current (ac) resistor and compensates for the resistive losses in the RLC circuit. Consequently, the TDO stabilizes the resonance, and with the aid of modern electronics, the resonant frequency (of order MHz) can be precisely measured.

There are several key aspects of the TDO-based method. Firstly, a stable bias voltage situated in the negative differential resistance region of the tunnel diode keeps a continuous positive feedback in the circuit. Secondly, a strict choice of inductor and capacitor is necessary, since the impedance ought to be comparable to the negative differential resistance of the tunnel diode, in order to replenish the dissipated energy. Thirdly, the internal resistance of the LC tank circuit should be as low as possible so as to minimize the damping of the circuit. Deviating from the required conditions leads to a rapid attenuation of the resonant oscillation.

Since the resonant frequency of an LC circuit is given by

$$f = \frac{1}{2\pi\sqrt{LC}}, \tag{1}$$

the physical properties of a given material can be studied, provided that the physical properties can couple to the inductance or capacitance. For solid materials, this coupling is typically achieved via coupling to an inductor through the mutual inductance.

A small change of the inductance ΔL directly corresponds to a shift of the resonant frequency f,

$$\Delta f = -\frac{\Delta L}{2\,L} f. \tag{2}$$

For an insulator, the inductance change is primarily related to the change in magnetic permeability: $\Delta L \sim g\frac{V_s}{V_c}\Delta\chi$, where g is a geometric factor, V_s/V_c is the volume ratio of the sample to coil, namely the filling factor, and $\Delta\chi$ is the change in the susceptibility. Therefore, the TDO-based method has been used to probe the magnetic susceptibility.[25,26]

For a metal, the presence of conduction electrons leads to eddy currents which shield the radio-frequency field from the bulk. Consequently, the inductance change is dominated by the change in skin depth. The skin depth is given by $d = (\pi f \mu\sigma)^{-1/2}$, where σ is the electrical conductance. The change in frequency is proportional to the change in skin depth: $\frac{\Delta f}{f} \sim -g\frac{\Delta d}{d}$. As a result, in metals the changes in frequency generally reflect the change of resistance (conductance).

While a superconductor in the Meissner state entirely excludes magnetic fields from the bulk, the field remains finite close to the surface of the superconductor. The length scale over which the field decreases beneath the surface of a superconductor is characterized by the London penetration depth, which is proportional to the change of resonant frequency, $\Delta\lambda = G\Delta f$, where $\Delta\lambda$ is the change of penetration depth with temperature or magnetic field, and G is a geometric factor which depends on the geometries of the sample and coil.[27] Since the penetration depth is related to the superfluid density n_s via the London equation $\lambda = [m/(n_s e^2\mu)]^{1/2}$, precise measurements of the temperature-dependent penetration depth using the TDO-based method can be used to probe the low energy excitations of a superconductor, and hence to determine the superconducting gap structure.

Here, we are interested in exploring the phase diagrams, Fermi surfaces, and topological properties of materials under the extreme conditions of high pressure, high magnetic fields and ultra-low temperatures. We focus in particular on strongly correlated electron systems, where emergent properties and unusual electronic phases are often revealed at low temperatures, upon tuning using pressure and/or magnetic fields. In order to use the TDO-based method under such conditions, a number of issues must be addressed. Firstly, using a large coil in the TDO circuit is beneficial to maintain the resonance but for high pressures, the volume of the coil and sample must be small, making it difficult to achieve a sufficient signal-to-noise ratio. Secondly, heating from the TDO circuit prevents the cryostat reaching very low temperatures.

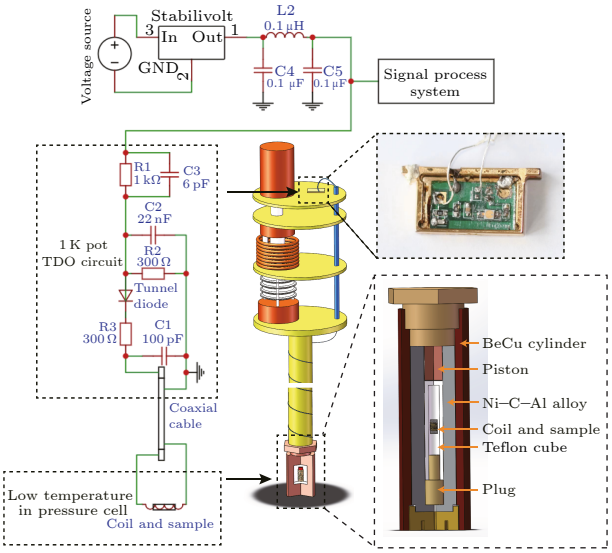

Fig. 1. Schematic diagram of our TDO-based measurement system with a dilution refrigerator. The coil and sample are placed in a pressure cell, which is connected to the TDO circuit at the 1 K pot by a coaxial cable.

The schematic of our TDO-based measurement system and the configuration of the pressure cell, circuit board and dilution refrigerator is displayed in Fig. 1. The coil in the previous setup[24] essentially had a fixed size because of the rigorous resonance condition. The selection of the resistor and capacitor in our new setup allows for a more flexible coil size while maintaining low noise levels. Our LC tank circuit is typically composed of a 100 pF mica chip capacitor and a sensor coil with 8–15 turns. If a smaller

coil inductor is required, we can utilize a smaller capacitor, allowing us to achieve a coil diameter of around 100 µm. For especially tiny samples, such as needle shape samples with a diameter smaller than 100 µm, a slightly different design is utilized, where both the resonant coil and capacitor are also cooled to low temperatures. This design can exclude the inductance and resistance of the coaxial cable from the LC resonant circuit so as to enhance the intrinsic signal from the sensor coil. Therefore, under a variety of conditions, we can ensure that the coil tightly encloses the sample, leading to a large filling factor, which maximizes the measured signal from the sample. The design is compatible with a wide range of resonant frequencies, from several MHz to nearly a GHz. Both the sample and coil can be placed in a piston cylinder pressure cell, which can be cooled in a ^{3}He refrigerator or dilution refrigerator. Using a piston pressure cell and Daphne 7373 as the pressure transmitting medium, we can achieve hydrostatic pressures up to 2.5 GPa. It should be noted that due to the lower power of the tunnel diode, the ac effective value is of the order of 100 µA. Consequently, the energy stored in the coil is relatively small, meaning that there is little heating arising from the ac magnetic field.

Besides the inductor coil, the other elements of the tunnel diode circuit are situated at the 1 K pot held at a temperature of around 1.6 K and are connected to the inductor via a low-impedance coaxial cable. This is primarily due to the heat produced by the circuit, which is counteracted by the 1 K pot. In addition, this allows for the temperature to be stabilized, and for magnetic fields to be avoided. We have introduced an additional capacitor and resistor to optimize the TDO circuit. R_3 connects to the tunnel diode in series, reducing the adverse influence of the parasitic capacitance of the tunnel diode. R_1 and R_2 allow for a stable DC bias voltage to be supplied for the whole low-temperature circuit and LC-tank circuit, respectively. Figure 1 shows the typical parameters for the different components. In addition, a large capacitor C_2 conducts the high-frequency signal while a small capacitor C_3 suppresses low-frequency signals, so as to eliminate noise from external circuits.

The components held at room temperature consist of the DC voltage source and the signal processing components. A voltage source with a stabilizer supplies a stable bias to the TDO circuit, which is vital for achieving a stable resonance, and is necessary for obtaining high-precision data with a noise level of less than 5 Hz in a hydrostatic pressure environment.

To date, measurements in magnetic fields up to 15 T and at pressures as high as 2.5 GPa have been performed using both an Oxford HelioxVL ^{3}He refrigerator with temperatures from 0.35 K to 20 K and a Kelvinox 400HA dilution refrigerator with temperatures from below 0.1 K to 0.8 K.

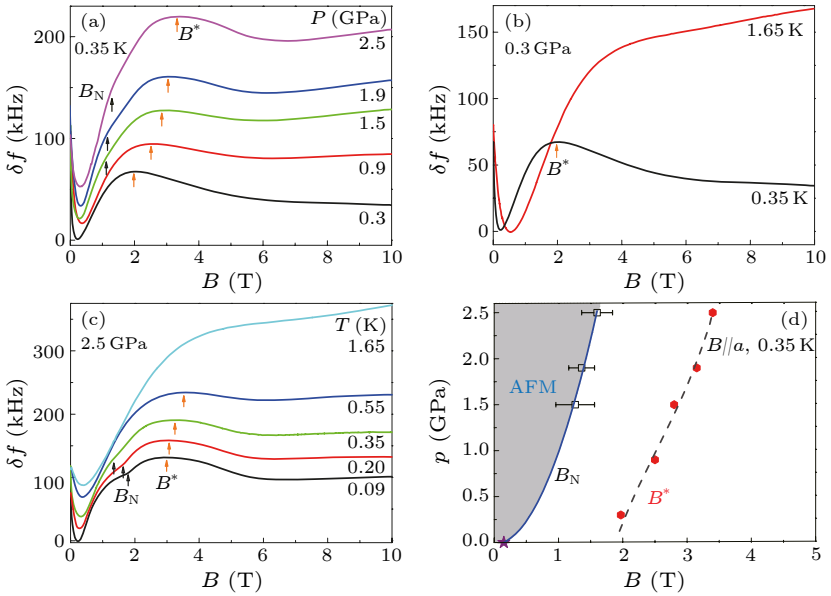

Fig. 2. Field dependence of the resonant frequency of YbPtBi measured using the TDO method (a) at 0.35 K at various pressures up to 2.5 GPa, where the data are shifted for clarity and δf is the difference between the resonant frequency f and the reference frequency f_r. The data are shown at several temperatures for (b) 0.3 GPa, and (c) 2.5 GPa. (d) The p–B phase diagram of YbPtBi for magnetic fields along [100] at 0.35 K. The data at ambient pressure indicated by the purple star is taken from Ref. [7].

Results and Discussion. Figure 2 displays the resonant frequency f of a single crystal of YbPtBi measured using the TDO method as a function of magnetic field applied along [100] for different pressures at 0.35 K, and at 0.3 GPa and 2.5 GPa for different temperatures. In experiments, we measure the difference δf between the resonant frequency f and a reference frequency f_r from the function generator. In all the displayed curves, δf decreases with increasing field at low fields, before reaching a minimum, above which there is a pronounced increase. This feature suggests that the TDO data is primarily a measure of the conductance, since this valley corresponds to the pronounced peak observed at low fields in the resistivity at ambient pressure.[7] A broad maximum B^* is also

observed upon further increasing the field, at around 1.9 T at 0.3 GPa, which moves to higher fields as the pressure increases. Furthermore, the broad maximum shifts to a higher field with increasing temperature and becomes less pronounced, eventually evolving into the shoulder feature observed at 1.65 K. The position of the local maximum at low pressure is close to the crossover field from non-Fermi liquid to Fermi liquid at ambient pressure,[7] above which the magnetoresistance has a weak field dependence. Therefore, B^* may correspond to the onset of the Fermi liquid behavior but the origin remains unclear and needs to be examined in future studies.

Under pressures of 1.5 GPa and above, a kink is observed below the broad maximum, indicated by the black arrows. The kink may correspond to a critical field B_N from the antiferromagnetic-to-paramagnetic phase, but this feature cannot be resolved at lower pressures potentially because the magnetic order has a too small moment at temperatures close to T_N to be detected, where it is also difficult to detect in the magnetoresistance at 0.35 K at ambient pressure.[7] Upon increasing the pressure, the kink moves to higher fields and becomes more pronounced, in line with the strengthening of magnetic order with applied pressure in Yb-based heavy fermion compounds. As shown in Fig. 2(c), upon decreasing the temperature at 2.5 GPa, the kink also becomes more distinct and moves to higher fields while B^* moves to lower fields. If the kink at B_N indeed corresponds to the breaking apart of long-range antiferromagnetic order, it suggests a rather significant increase of the critical field from 0.4 T to 1.8 T,[7] despite there only being a moderate enhancement of T_N at low pressures.[11] From neutron diffraction measurements at ambient pressure, short-range antiferromagnetic order is found to persist above B_N up to around 1 T at 0.35 K, so the significant increase of B_N is possibly related to a change from short-range to long-range order under pressure.[8] These result are in line with those typically found for Yb-based heavy fermion compounds under pressure, since pressure enhances the strength of the RKKY interaction relative to the Kondo effect, enhancing magnetic order and leading to more localized $4f$ electrons.[28–31]

In the high field region, distinct quantum oscillations are observed. Figure 3(a) displays the quantum oscillations between 10 and 15 T at different pressures at 0.35 K, where a background polynomial term has been subtracted. The oscillation frequencies were extracted by performing fast Fourier transforms (FFT), and the results are displayed in Fig. 3(b), where the frequencies are proportional to the extremal cross-sectional areas of the Fermi surface perpendicular to the magnetic field. The frequencies labelled α, β, δ, γ and η at 0.3 GPa correspond to those observed in previous quantum oscillation measurements at ambient pressure.[32] Slight differences between the frequency values can be attributed to the application of a small pressure in the present study, as well as slight deviations in the direction of the applied field. In addition, we find three additional frequencies labeled ε, ζ and θ, which were not observed in the previous report. However, the frequency θ is only found at several pressures. Figure 3(c) shows the evolution of the major FFT frequencies with pressure. With increasing pressure, all the frequencies show a slight decrease. Since the oscillation frequencies are proportional to the extremal cross-sectional areas of the Fermi surface, such a decrease of all frequencies indicates that the Fermi surface volume decreases with pressure. These results are consistent with the $4f$ electrons becoming increasingly localized with pressure, and hence their contribution to the Fermi surface is reduced.

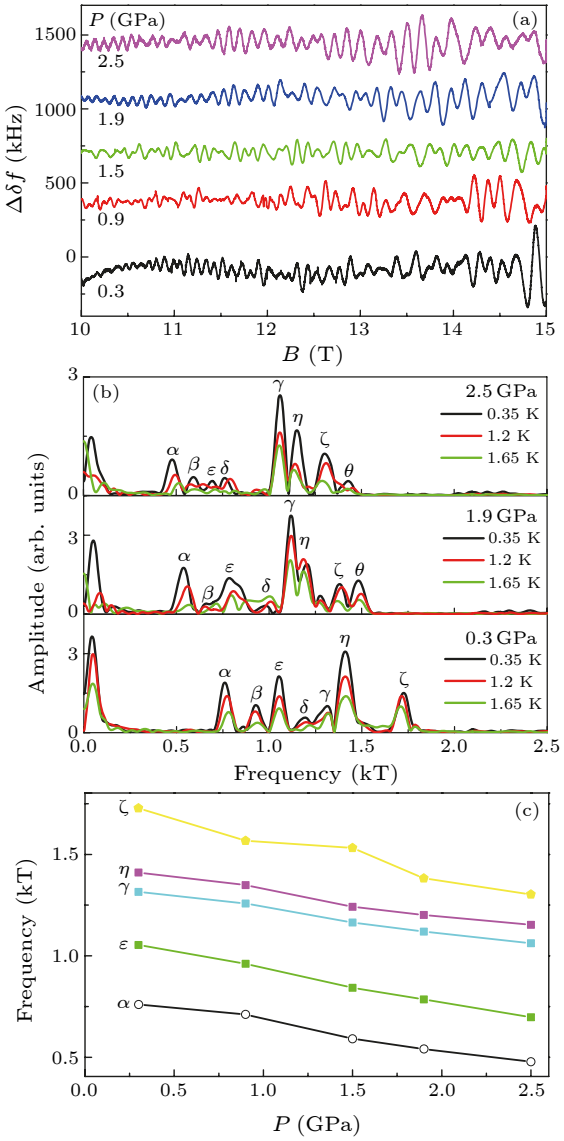

Fig. 3. Quantum oscillations of YbPtBi (a) under different pressures at 0.35 K for magnetic fields applied along [100], where $\Delta\delta f$ corresponds to the frequency shift after subtracting the background contribution. (b) FFT of the data taken at different pressures at several temperatures. (c) The evolution of the frequencies α, ε, γ, η and ζ with pressure.

Figures 4(a) and 4(b) display quantum oscillations at 2.5 GPa at different temperatures measured in a ^{3}He refrigerator and a dilution refrigerator, respectively. The corresponding FFT results are displayed in Figs. 5(a) and 5(b), which show a close correspondence between measurements in the two refrigerators. Here the small differences in the frequency values are likely due to slightly different directions of the applied field. From examining the FFT results at different temperatures, in Fig. 5(a) it can be seen

that at 2.5 GPa there is an abrupt change in the amplitudes corresponding to the γ, η, ζ and δ frequencies below $T' \approx 0.6$ K. A similar change is found approximately at 0.45 K for 1.9 GPa, and at 0.35 K for 1.5 GPa. Remarkably, T' is approximately identical to T_N, so there may be a relationship between the magnetic ordering and the anomalous change in quantum oscillations. In addition, the frequency values of η, ζ, δ and β slightly shift with temperature, suggesting a slight change in the areas of their orbits. The temperature dependence of the amplitudes of the η and γ components at 0.9 and 2.5 GPa are shown in Figs. 5(c) and 5(d). Quantum oscillation amplitudes generally decrease with temperature following the Lifshitz–Kosevich (LK) formula,[33] $A = A_0(14.69m^*T/B)/[\sinh(14.69m^*T/B)]$, where m^* is the effective carrier mass, and B is the average inverse-field of the FFT window. At 0.9 GPa, the temperature dependence of the amplitudes can be well described by the LK formula, as shown by the solid lines. The fitted effective masses are $m^* = 0.92m_e$ and $1.04m_e$ for η and γ, respectively. However, at 2.5 GPa, the amplitudes can only be described by the LK formula at temperatures above T', whereas there is an abrupt change below. The fitted effective masses show no obvious change as the pressure increases. On the other hand, the abrupt change below T' corresponds to a deviation from the LK formula. An anomalous low temperature change in quantum oscillation amplitudes was observed in some strongly correlated systems such as SmSb,[34] SmB_6,[35] $CeCoIn_5$[36] and heterostructures of α-$RuCl_3$ on graphene.[37] There is a particular similarity to the case of SmSb, where the significant change of amplitude also occurs around the antiferromagnetic ordering temperature. However, the long-range and short-range magnetic orderings of YbPtBi are both destroyed in a 10 T field at ambient pressure,[8] so further experiments under pressure are necessary to determine the origin of this behavior.

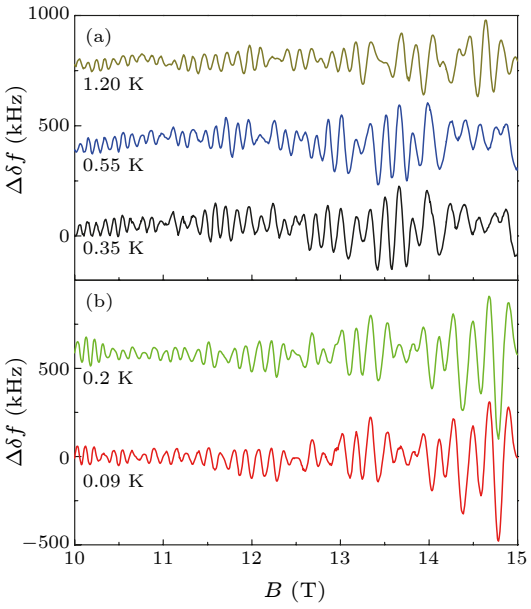

Fig. 4. Quantum oscillations of YbPtBi at various temperatures at 2.5 GPa measured in (a) the ^{3}He refrigerator and (b) the dilution refrigerator, where $\Delta\delta f$ corresponds to the frequency shift after subtracting the background contribution.

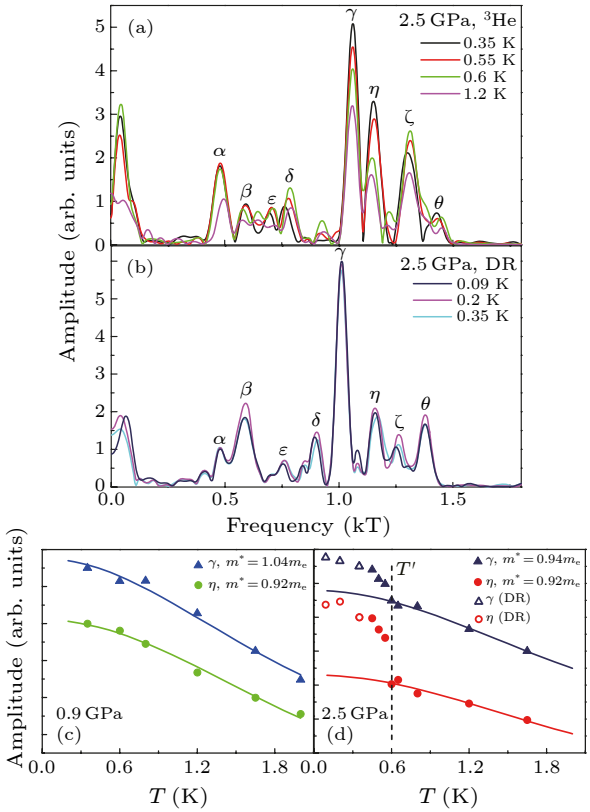

Fig. 5. The corresponding FFT results of the quantum oscillations measured in (a) the ^{3}He refrigerator and (b) the dilution refrigerator. The temperature dependence of the oscillation amplitudes for two frequencies are shown at (c) 0.9 GPa, and (d) 2.5 GPa. The solid lines show the results from fitting with the LK formula, which at 0.9 GPa can describe the behavior across the whole temperature range, while at 2.5 GPa there is an anomalous change at T', indicated by a dashed line. All data and fitted curves are normalized and shifted for clarity.

In summary, we have probed the evolution of the physical properties of the heavy fermion antiferromagnet YbPtBi under pressure using TDO-based measurements, in which we have modified our experimental setup to enable us to measure under the extreme conditions of low temperatures, high pressures, and high magnetic fields, without compromising the signal-to-noise ratio. We construct a low temperature p–B phase diagram for YbPtBi, which suggests that there is an increasing robustness of long-range antiferromagnetic order under pressure. We also track the evolution of the quantum oscillations up to 2.5 GPa, and observe additional quantum oscillation frequencies not reported in the previous Shubnikov–De Haas effect study at ambient pressure,[32] demonstrating the high sensitivity of our technique under pressure. The results show a reduction of all the oscillation frequencies with pressure, pointing to the shrinking of the Fermi surface and an increasing localization of the Yb $4f$ electrons. Moreover, an abrupt change is observed in the quantum oscillation amplitudes above 1.5 GPa below around T_N, while understanding the origin of this behavior requires further experiments.

Acknowledgments. This work was supported by the National Key Research and Development Program of

China (Grant No. 2017YFA0303100), the National Natural Science Foundation of China (Grant Nos. 11974306 and 12034017), and the Natural Science Foundation of Zhejiang Province (Grant No. 2021C01002).

References

[1] Gegenwart P, Si Q, and Steglich F 2008 *Nat. Phys.* **4** 186

[2] Zhou X, Lee W S, Imada M, Trivedi N, Phillips P, Kee H Y, Törmä P, and Eremets M 2021 *Nat. Rev. Phys.* **3** 462

[3] Pei C, Xia Y, Wu J, Zhao Y, Gao L, Ying T, Gao B, Li N, Yang W, Zhang D, Gou H, Chen Y, Hosono H, Li G, and Qi Y 2020 *Chin. Phys. Lett.* **37** 066401

[4] Xia X B, Shen B, Smidman M, Chen Y, Lee H, and Yuan H Q 2018 *Chin. Phys. Lett.* **35** 067102

[5] Xu J C, Su H, Kumar R, Luo S S, Nie Z Y, Wang A, Du F, Li R, Smidman M, and Yuan H Q 2021 *Chin. Phys. Lett.* **38** 087101

[6] Fisk Z, Canfield P C, Beyermann W P, Thompson J D, Hundley M F, Ott H R, Felder E, Maple M B, de Lopez L T M A, Visani P, and Seaman C L 1991 *Phys. Rev. Lett.* **67** 3310

[7] Mun E D, Bud'ko S L, Martin C, Kim H, Tanatar M A, Park J H, Murphy T, Schmiedeshoff G M, Dilley N, Prozorov R, and Canfield P C 2013 *Phys. Rev. B* **87** 075120

[8] Ueland B G, Kreyssig A, Mun E D, Lynn J W, Harriger L W, Pratt D K, Prokeš K, Hüsges Z, Toft-Petersen R, Sauerbrei S, Saunders S M, Furukawa Y, Bud'ko S L, McQueeney R J, Canfield P C, and Goldman A I 2019 *Phys. Rev. B* **99** 184431

[9] Guo C Y, Wu F, Wu Z Z, Smidman M, Cao C, Bostwick A, Jozwiak C, Rotenberg E, Liu Y, Steglich F, and Yuan H Q 2018 *Nat. Commun.* **9** 4622

[10] Guo C, Wu F, Smidman M, and Yuan H 2018 *AIP Adv.* **8** 101336

[11] Lacerda A, Movshovich R, Hundley M F, Canfield P C, Arms D, Sparn G, Thompson J D, Fisk Z, Fisher R A, Phillips N E, and Ott H R 1993 *J. Appl. Phys.* **73** 5415

[12] Van Degrift C T 1975 *Rev. Sci. Instrum.* **46** 599

[13] Van Degrift C T and Love D P 1981 *Rev. Sci. Instrum.* **52** 712

[14] Prozorov R and Giannetta R W 2006 *Supercond. Sci. Technol.* **19** R41

[15] Yuan H Q, Agterberg D F, Hayashi N, Badica P, Vandervelde D, Togano K, Sigrist M, and Salamon M B 2006 *Phys. Rev. Lett.* **97** 017006

[16] Weng Z F, Zhang J L, Smidman M, Shang T, Quintanilla J, Annett J F, Nicklas M, Pang G M, Jiao L, Jiang W B, Chen Y, Steglich F, and Yuan H Q 2016 *Phys. Rev. Lett.* **117** 027001

[17] Pang G, Smidman M, Zhang J, Jiao L, Weng Z, Nica E M, Chen Y, Jiang W, Zhang Y, Xie W, Jeevan H S, Lee H, Gegenwart P, Steglich F, Si Q, and Yuan H 2018 *Proc. Natl. Acad. Sci. USA* **115** 5343

[18] Duan W, Nie Z, Luo S, Yu F, Ortiz B R, Yin L, Su H, Du F, Wang A, Chen Y, Lu X, Ying J, Wilson S D, Chen X, Song Y, and Yuan H 2021 *Sci. Chin. Phys. Mech. & Astron.* **64** 107462

[19] Coffey T, Bayindir Z, DeCarolis J F, Bennett M, Esper G, and Agosta C C 2000 *Rev. Sci. Instrum.* **71** 4600

[20] Sebastian S E, Harrison N, Liang R, Bonn D A, Hardy W N, Mielke C H, and Lonzarich G G 2012 *Phys. Rev. Lett.* **108** 196403

[21] Wang A, Du F, Zhang Y, Graf D, Shen B, Chen Y, Liu Y, Smidman M, Cao C, Steglich F, and Yuan H 2021 *Sci. Bull.* **66** 1389

[22] Lin W C, Campbell D J, Ran S, Liu I L, Kim H, Nevidomskyy A H, Graf D, Butch N P, and Paglione J 2020 *npj Quantum Mater.* **5** 68

[23] Ran S, Saha S R, Liu I L, Graf D, Paglione J, and Butch N P 2021 *npj Quantum Mater.* **6** 75

[24] Zhang J 2014 *Ph.D. Dissertation* (Hangzhou: Zhejiang University)

[25] Clover R B and Wolf W P 1970 *Rev. Sci. Instrum.* **41** 617

[26] Vannette M D, Sefat A S, Jia S, Law S A, Lapertot G, Bud'ko S L, Canfield P C, Schmalian J, and Prozorov R 2008 *J. Magn. Magn. Mater.* **320** 354

[27] Prozorov R, Giannetta R W, Carrington A, and Araujo-Moreira F M 2000 *Phys. Rev. B* **62** 115

[28] Yuan H Q, Nicklas M, Hossain Z, Geibel C, and Steglich F 2006 *Phys. Rev. B* **74** 212403

[29] Jiang W B, Yang L, Guo C Y, Hu Z, Lee J M, Smidman M, Wang Y F, Shang T, Cheng Z W, Gao F, Ishii H, Tsuei K D, Liao Y F, Lu X, Tjeng L H, Chen J M, and Yuan H Q 2015 *Sci. Rep.* **5** 17608

[30] Salamatin D A, Sidorov V A, Chtchelkatchev N M, Magnitskaya M V, Martin N, Petrova A E, Fomicheva L N, Guo J, Huang C, Zhou Y, Sun L, and Tsvyashchenko A V 2021 *Phys. Rev. B* **103** 235139

[31] Matsubayashi K, Hirayama T, Yamashita T, Ohara S, Kawamura N, Mizumaki M, Ishimatsu N, Watanabe S, Kitagawa K, and Uwatoko Y 2015 *Phys. Rev. Lett.* **114** 086401

[32] Mun E, Bud'ko S L, Lee Y, Martin C, Tanatar M A, Prozorov R, and Canfield P C 2015 *Phys. Rev. B* **92** 085135

[33] Shoenberg D 1984 *Magnetic Oscillations in Metals* (Cambridge: Cambridge University Press)

[34] Wu F, Guo C, Smidman M, Zhang J, Chen Y, Singleton J, and Yuan H 2019 *npj Quantum Mater.* **4** 20

[35] Tan B S, Hsu Y T, Zeng B, Hatnean M C, Harrison N, Zhu Z, Hartstein M, Kiourlappou M, Srivastava A, Johannes M D, Murphy T P, Park J H, Balicas L, Lonzarich G G, Balakrishnan G, and Sebastian S E 2015 *Science* **349** 287

[36] Shishido H, Yamada S, Sugii K, Shimozawa M, Yanase Y, and Yamashita M 2018 *Phys. Rev. Lett.* **120** 177201

[37] Mashhadi S, Kim Y, Kim J, Weber D, Taniguchi T, Watanabe K, Park N, Lotsch B, Smet J H, Burghard M, and Kern K 2019 *Nano Lett.* **19** 4659